2017

Effect of Atmospheric Transmittance on Performance of Adaptive SPD-vacuum Switchable Glazing

Aritra Ghosh
University of Exeter

Brian Norton
Technological University Dublin, brian.norton@tudublin.ie

Aidan Duffy
Technological University Dublin, aidan.duffy@tudublin.ie

Recommended Citation

Ghost, A., Norton, B. & Duffy, A. (2017). Effect of atmospheric transmittance on performance of adaptive SPD-vacuum switchable glazing. *Solar Energy Materials and Solar Cells*, vol. 161, pg. 424-431. doi:10.1016/j.solmat.2016.12.022

Effect of atmospheric transmittance on performance of adaptive SPD-vacuum switchable glazing

Aritra Ghosh*

aritra.ghosh@mydit.ie

aritraghosh_9@yahoo.co.in

Brian Norton

Aidan Duffy

Dublin Energy Lab, Dublin Institute of ~~Technology~~Technology, ~~Dublin~~Dublin, Ireland

*Corresponding author.

Abstract

Combined suspended particle device (SPD)-vacuum glazing is a potential adaptive glazing for low energy building application. Glazing transmission is an essential parameter to determine indoor comfort level of building due to glazing. In this work, above 0.5 clearness index, a strong correlation between glazing transmission and clearness index (Atmospheric transmission) has been evaluated for south facing vertical plane glazing. Below 0.5 clearness index, isotropic diffuse transmittance was dominant and one single value of glazing transmission was found which is suitable for building energy calculation throughout the year. Below 0.5 clearness index, for south facing vertical plane SPD-vacuum glazing transmission was 17% and 1.1% for transparent and opaque states respectively.

Keywords: Adaptive; ~~glazing~~Glazing; ~~clearness~~Clearness index; ~~vacuum~~Vacuum; SPD; ~~transmission~~Transmission; ~~solar~~Solar heat gain coefficient

Nomenclature

A_i

Anisotropy index

$I_{beam,h}$

Horizontal plane beam solar radiation (W/m^2)

$I_{dif,h}$

Horizontal plane beam solar radiation (W/m^2)

$I_{global,h}$

Horizontal plane global solar radiation (W/m^2)

$I_{global,v}$

Vertical plane global solar radiation (W/m^2)

I_{extra}

Extra-terrestrial solar radiation (W/m^2)

I_{sc}

Solar constant (W/m^2)

k_d

Diffuse factor

k_T

Clearness index

n_g

Refractive index of SPD glazing

N_g

Number of glass pane

SHGC

Solar heat gain coefficient

SE

Transmitted solar energy (W/m2)(W/m^2)

Greek symbols

α_g

Absorptance

τ

Transmittance

τ_v

Vertical global transmittance

τ_{dir}

Direct transmittance

τ_{diff}

Diffuse transmittance

θ

Incident angle

β

Slope angle

1 Introduction

To achieve 90% less CO_2 emission from building in 2050 compared to 1990 new innovative building technologies are required [1] which will lower CO_2 emission, reduce energy demand, and maintain indoor environment quality based on occupant choice [2]. Thus, building envelopes are key contributor to regulate the heat and mass transfer between the outdoor and indoor environment. In a building, glazing is the weakest part as solar heat gain admitted through it and heat loss occurs mostly through it. To follow the building directives, new adaptive glazing technologies are required which will enhance to achieve the targets. The development of adaptive building envelope technologies, and particularly of switchable glazing, can make significant contributions to decarbonisation targets [3,4].

Available adaptive glazing technologies [5–8] are electrochromic (EC) [9–11], suspended particle device (SPD) [12–15], liquid crystal (LC) [16,17], thermochromic [18,19], thermotropic [20,21], phase change material (PCM) [22–25], gasochromic [26,27], aerogel [28,29], and vacuum [30]. These glazing are classified in two groups-

- solar heat gain control glazing which change its transparency by electrical (EC,SPD,LC), heat (thermotorpic, PCM) or chemical (gasochromic, thermochromic) actuation;
- low heat loss glazing (aerogel, vacuum, low e coating) which has constant transparency and due to presence of vacuum or insulating material, heat loss through glazing is low.

Electrically actuated solar heat gain control glazings are advantageous over non electrically actuated glazing as they are controlled by occupant choice. SPD glazing as shown in Fig. 1 is advantageous over EC as it is powered by alternating current (AC) power supply which enable it to connect directly with main household power supply, no power is required to achieve opaque states and it is clear compared to LC [31]. SPD glazing is an AC powered glazing changes its state from “opaque” to transparent for the applied voltages change from 0 to 110 V, 0.007 W [32]. Outdoor characterisation of SPD glazing using test cell investigation showed that SPD glazing has overall heat transfer coefficient (*U*-value) nearly 5.9 W/m^2K [15]. Solar heat gain coefficient of SPD glazing varied between 0.5 and 0.55 [33]. SPD glazing is a potential device to control glare [34]. However, SPD single glazing is suitable for hot climatic and summertime. It has less potential to control the heat loss from room to ambient due to its high *U*-value [33].

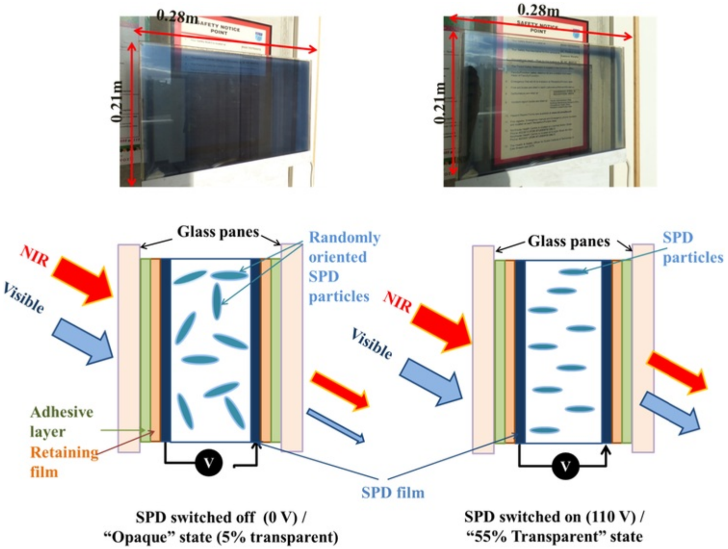

Fig. 1 Schematic details of suspended particle device switchable glazing “opaque” and “transparent” state.

alt-text: Fig. 1:

Due to variation of weather throughout the year, heat loss and heat control both are essential in a glazing to achieve low energy building. During winter, low heat loss glazings are advantageous as they limit the losses through glazing from inside a room to outside. Vacuum glazing shown in Fig. 2 is a potential low heat loss glazing due to its nearly clear transparency similar to double-glazing though 53% less heat transmit through it [35]. Vacuum glazing possesses nearly 1.14 W/m^2K overall heat losses, which is 80% lower than a SPD glazing [35]. However, vacuum glazing has no potential to control glare as it allows equal amount of illuminance compared to double glazing [35]. Addition of vacuum and SPD glazing will act as a switchable vacuum glazing or low heat loss SPD glazing as shown in Fig. 3. This glazing has solar heat gain control and heat loss control potential as reported by Ghosh et.al. [36].

(a)

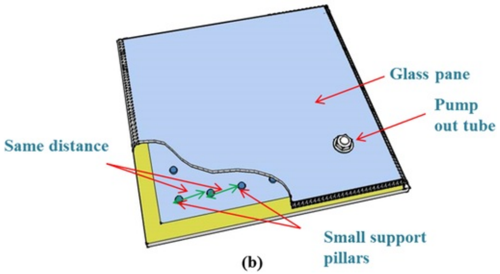

(b)

Fig. 2 (a) ~~photograph~~Photograph of a NSG SPAICA vacuum glazing, (b) schematic top view of vacuum glazing.

alt-text: Fig. 2

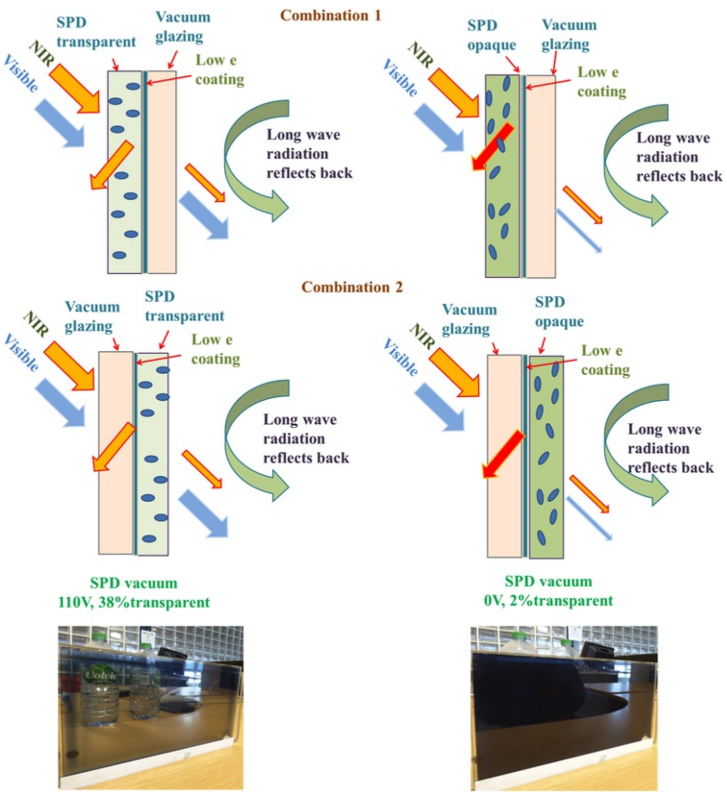

Fig. 3 Detail of a combined SPD–vacuum glazing in its opaque and transparent states.

alt-text: Fig. 3:

Low heat loss switchable SPD glazing is a potential device for future adaptive glazing for building application. Transmission of glazing varies with incident angle. Thus, accurate glazing transmission determination is a crucial factor as glazing transmission available from commercial provider is only suitable for normal incidence. In solar energy calculation, solar radiation data get higher priority than incident angle. Solar radiation measurement in a particular location needs global solar radiation and direct or diffuse solar radiation. Clearness index replace the necessity of different measured solar radiation data, as it only requires global horizontal solar radiation data. Dependency of clearness index and glazing transmission will be path breaking for future building application where only one measured data can predict the glazing transmission, transmitted solar energy, and solar heat gain coefficient. Theoretically, relation between glazing transmission and clearness index was investigated by Waide and Norton [37]. In this work first time dependency of clearness index and SPD-vacuum glazing performance has been experimentally evaluated. These results will reduce the tedious calculation for building engineer and architecture.

2 Methodology

For vertical plane SPD-vacuum glazing, angular transmittance τ_v (global solar transmittance through glazing) can be written as [33,35,36] Eq. (1).

$$\tau_v = \left[k_d \left\{k_T R_b \left(1 - k_d\right) + (1 - \cos \beta) \left(1 - k_T \left(1 - k_d\right)\right)\right\} + R_b \left(1 - k_d\right) + R_g \frac{1 - \cos \beta}{2}\right] \times \tau_{dir} R_b \left(1 - k_d\right) \left(1 + k_d k_T\right) + \frac{\tau_{dif} k_d}{2} (1 + \cos \beta) \left(1 - k_T \left(1 - k_d\right)\right) + \frac{\tau_g R_{g(1 - \cos \beta)}}{2} \quad (1)$$

where

$$\tau = \frac{1}{2}\left[\frac{1-\left\{\frac{\sin(\theta-n)}{\sin(\theta+n)}\right\}^2}{1+\left(2n_g-1\right)\left\{\frac{\sin(\theta-n)}{\sin(\theta+n)}\right\}} + \frac{1-\left\{\frac{\tan(\theta-n)}{\tan(\theta+n)}\right\}^2}{1+\left(2n_g-1\right)\left[\frac{\tan(\theta-n)}{\tan(\theta+n)}\right]^2}\right] \times \exp\left(\frac{-k_g N_g t_g}{\cos\ \theta}\right) \quad (2)$$

~~and~~and

$\tau = \tau_{dir}$ when $\theta = \theta_{dir}$

$\tau = \tau_{dif}$ when $\theta = \theta_{dif} = 59.68 - 0.1388\ \beta + 0.001497\ \beta^2$ [38]

$\tau = \tau_g$ when $\theta = \theta_g = 90 - 0.5788\beta + 0.002693\beta^2$ [38]

and diffuse factor (k_d) and clearness index (k_T) can be written as Eqs. (3) and (4) respectively.

$$k_d = \frac{I_{dif,h}}{I_{global,h}} \quad (3)$$

$$k_T = \frac{I_{global,h}}{I_{extra}} \quad (4)$$

Solar energy (SE) transmitted through SPD-vacuum glazing can be written as Eq. (5)[36]

$$SE = \left(I_{beam,h} + I_{dif,h}A_i\right)\tau_{dir}R_b + I_{dif,h}\left(1+A_i\right)\tau_{dif}\frac{(1+\cos\ \beta)}{2} + I_{global,h}\rho_g\tau_g\frac{(1-\cos\ \beta)}{2} \quad (5)$$

~~Where~~where anisotropic index A_i can be written by Eq. (6)

$$A_i = \frac{I_{beam,h}}{I_{extra}} \quad (6)$$

$$I_{extra} = I_{sc}\left(1 + 0.033\ \cos\ \frac{360n}{365}\right)(\cos\ \phi\ \cos\ \delta\ \cos\ \omega + \sin\ \phi\ \sin\ \delta) \quad (7)$$

I_{sc} is the solar constant, n is the day of year, ϕ latitude angle, δ declination angle ω hour ~~angle~~angle.

Dynamic solar heat gain coefficients (SHGC) can be evaluated by Eq. (8)[36]

$$SHGC = \frac{SE}{I_{global,v}} \quad (8)$$

3 Experiment

One SPACIA vacuum glazing from Nippon Sheet Glass and SPD glazing from smart glass international were employed in this experiment. These two glasses were attached together to obtain low heat loss switchable SPD glazing. Edges of the combined glazing were sealed by silicon. Details of glazing are listed in Table 1. Details of experiment procedures are described in [33,35,36]. Hemispherical transmission spectrum of the SPD-vacuum glazing was performed using AvaSpec-ULS2048L Star Line Versatile Fiber-optic spectrometer under indoor condition. A Kipp and Zonen model SMP11 pyranometer was used to measure global solar radiation incident on the vertical surface. Fig. 4 represents the SPD-vacuum glazing normal hemispherical transmission spectra for transparent and opaque state. After 800 nm the transmitted infra radiation is higher compare to visible wavelength.

Table 1 Details of glazings.

alt-text: Table 1:

	Solar transmission (278–1100 nm)	Visible transmission (380–780 nm)	Power	Supplier
SPD transparent (switch on)+vacuum	39	38	110 V, 0.007 W	Smart glass international (Dublin, Ireland), NSG SPACIA (UK)
SPD opaque (switch off)+vacuum	10	2	0 V	

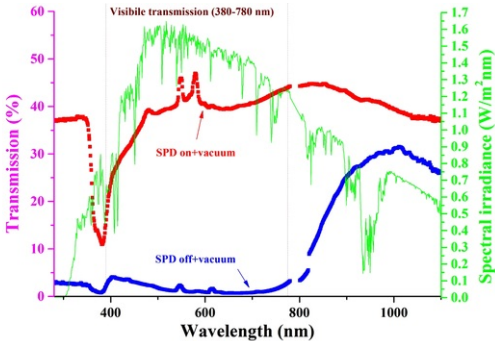

Fig. 4 Transmission spectra of SPD glazing “opaque” and “transparent” states.

alt-text: Fig. 4

4 Results & discussion

Diurnal variation of calculated clearness index, diffuse factor and anisotropy index, transmitted solar energy through SPD-vacuum glazing for its “transparent” and “opaque” state and measured vertical surface solar radiation for clear sunny, intermittent cloudy and overcast cloudy day are shown in Fig. 5. Transmitted solar energy was calculated using Eq. (5). Clearness index, which represent global solar radiation transmission, was achieved maximum 0.8 at mid-day period for a clear sunny day. Anisotropy index (A_i) was 0.7, which represents atmosphere transmittance for the direct solar radiation. Higher values of A_i and k_T and lower k_d indicate that the global radiation is mostly direct solar radiation for a clear sunny day. At mid-day time during 0.8 clearness index, diffuse fraction values were low nearly 0.3 which represents that the diffuse radiation at this time was lower compare to direct solar radiation. For intermittent and overcast day lower clearness index and lower anisotropic index was achieved where as higher values of diffuse factor was obtained. 76% higher Maximum transmitted solar energy was possible for SPD-vacuum glazing transparent state compared to opaque state under 955 W/m^2 solar radiation in a typical clear sunny day.

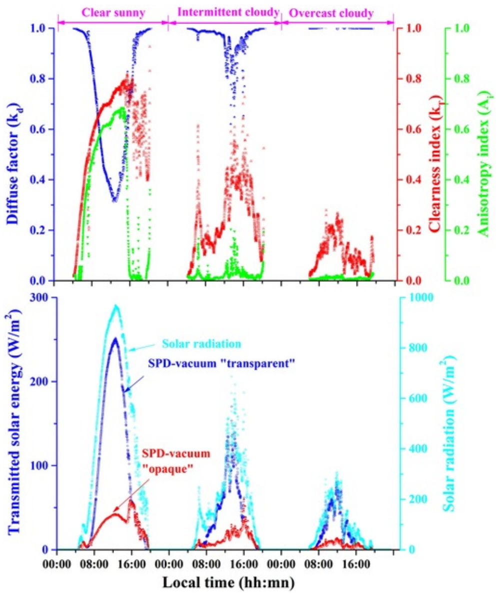

Fig. 5 Diurnal variation of calculated clear ness index, diffuse fraction, anisotropy index, and transmitted solar energy through SPD-vacuum glazing and measured vertical surface solar radiation for clear sunny, intermittent cloudy and overcast cloudy day.

alt-text: Fig. 5:

Fig. 6 represents the variation of glazing transmission for varying incident angle. Two different days were considered ~~1~~1st~~st~~ of July and ~~1~~1st~~st~~ of January to measure the SPD-vacuum glazing transmission for its transparent and opaque state. In Dublin location, for south facing vertical plane glazing it is evident that the incident angle varies between 13° ~~to 82~~and 82°.~~0~~ In January, glazing transmission is higher compared to transmission in July.

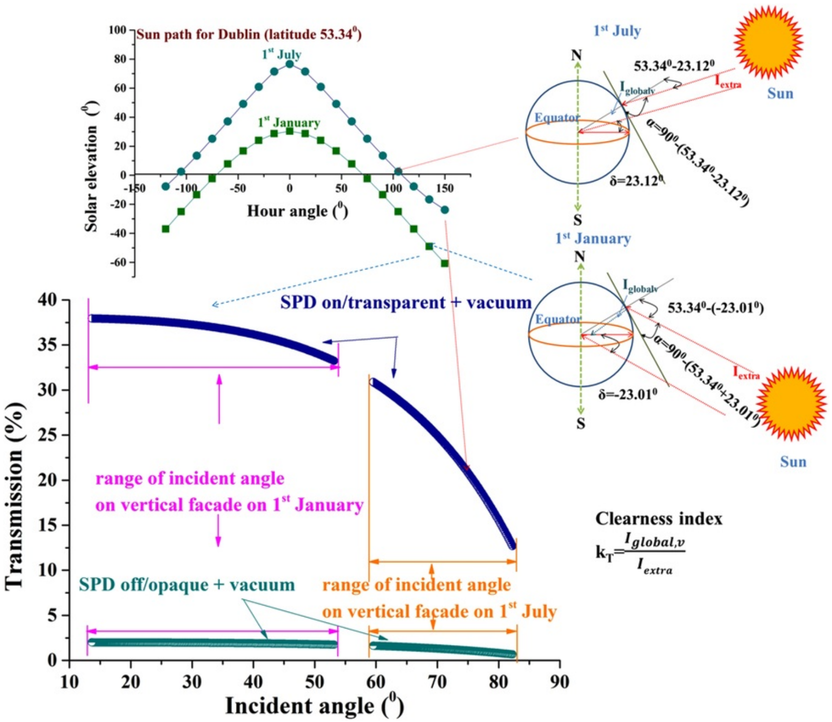

Fig. 6 Variation of transparent SPD-vacuum glazing transmission (38%) for different incident angle on ~~1~~1st~~st~~ of July while the sun ray strike the ground on at an angle 59.78° and opaque SPD-vacuum glazing transmission (2%) for different incident angle on ~~1~~1st~~st~~ of January while the sun ray strike the ground on at an angle 13.65° in Dublin.

alt-text: Fig. 6

Correlation between measured south facing glazing transmission and clearness index is represented in Fig. 7. Below 0.5 clearness index, glazing transmission was low and domination of isotropic diffuse transmittance was observed for south facing glazing. Above 0.5 clearness index, angular direct transmission was dominant and a strong linear correlation between glazing transmission and clearness index was found. For south facing glazing, one single glazing transmission value can be used below 0.5 clearness index [37], to reduce the building simulation time and complexity. For vertical plane south facing transparent SPD-vacuum glazing, below 0.5 clearness index 17% glazing transmission is acceptable for designing and calculation purpose. For opaque SPD-vacuum glazing, under same conditions, acceptable transmittance value is 1.1%. Below 0.5 clearness index, these values can be used for building design calculation throughout the year, which will offer only less than 1% error. This glazing transmission is applicable for other azimuthal directions though the threshold values of clearness index changes. Table 2 listed the different clearness index for different azimuthal directions.

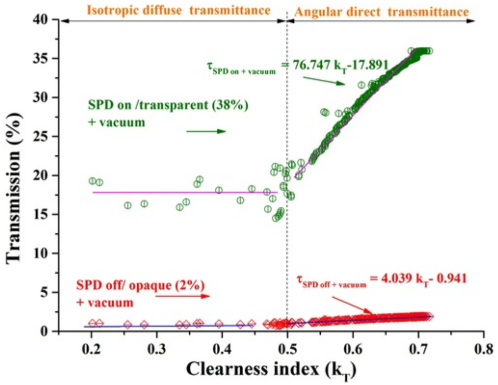

Fig. 7 Variation of south facing combined SPD-vacuum glazing transmission for its opaque and transparent state with clearness index.

alt-text: Fig. 7

Table 2 Yearly usable single glazing transmission value for SPD-vacuum transparent and opaque state.

alt-text: Table 2:

	Azimuthal direction	SPD on/transparent+vacuum (38% transparent) transmission	SPD off/opaque+vacuum (2% transparent) transmission	Mean monthly clearness index
	North	17	1.1	0.7
	South	17	1.1	0.5
Vertical plane SPD-vacuum glazing	East	17	1.1	0.6
	West	17	1.1	0.6
	North east	17	1.1	0.6
	North west	17	1.1	0.6

Fig. 8 shows the correlation between clearness index and solar heat gain coefficient (SHGC). Strong linear correlation above 0.5 clearness index was observed. Below 0.5 clearness index, SHGC of south facing vertical plane SPD vacuum glazing were 0.08 and 0.03 for its transparent and opaque states respectively. From Eq. (8), it is evident that SHGC is directly related to the glazing transmittance. Thus, these single values can be considered yearly usable for south facing vertical plane glazing. Mean monthly clearness index values changes with different azimuthal orientation. To eliminate complex calculation a particular threshold clearness index and SHGC for that clearness index for different orientation has been listed in Table 3.

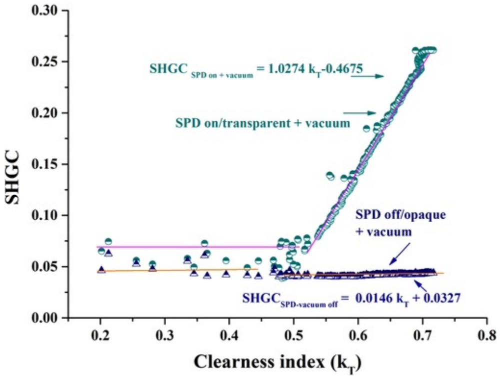

Fig. 8 Variation of solar heat gain coefficient with clearness index.

alt-text: Fig. 8:

Table 3 Yearly usable single SHGC value for SPD-vacuum transparent and opaque state.

alt-text: Table 3

	Azimuthal direction	SPD on (38% transparent)+vacuum SHGC	SPD off (2% transparent)+vacuum SHGC	Mean monthly clearness index
	North	0.08	0.03	0.7
	South	0.08	0.03	0.5
Vertical plane SPD-vacuum glazing	East	0.08	0.03	0.6
	West	0.08	0.03	0.6
	North east	0.08	0.03	0.6
	North west	0.08	0.03	0.6

Fig. 9 represents the correlation between clearness index and transmitted solar energy through the glazing for its two different states. Below clearness index 0.5, transmitted solar energy for south facing vertical plane SPD-vacuum glazing for its opaque and transparent states were 11 W/m^2 and 21 W/m^2. Table 4 shows the threshold clearness index for different azimuthal direction. Below this threshold clearness index, yearly usable single transmitted values can be applicable for building design calculation, which will offer less than 1% calculation error. 5ConclusionsCombined SPD-vacuum is a potential device for adaptive glazing application. Transparency of adaptive switchable glazing is an important factor as it decides the solar heat gain and indoor comfort of a building. Correlation between clearness index and glazing transmission, transmitted solar energy and solar heat gain coefficients has been evaluated for adaptive low heat loss switchable SPD glazing in its “transparent” and “opaque” state. From results, it is confirmed that glazing transmittance is directly influenced by sky condition. As clearness index needs only one measured parameter, correlation between clearness index and glazing transmittance will easier the calculation process. Isotropic diffuse transmittance is dominant while clearness index is below 0.5. Below 0.5 clearness index, for south facing vertical plane SPD-vacuum glazing's transmissions were 1.1% and 17% for its opaque and transparent state respectively. Above 0.5 clearness index, direct insolation was dominant and a linear correlation was found between clearness index and glazing transmission. This study offers a yearly usable single glazing transmittance, transmitted solar energy, solar heat gain coefficient for SPD-vacuum glazing in transparent and opaque state, which is advantageous for the building designers in northern latitude areas.AcknowledgementsThe work described in this paper was supported by the Graduate Research Education Programme of the Higher Education Authority, Ireland.The authors would also like to thank the anonymous reviewers for their constructive comments that helped to improve the manuscript. (Please seperate the conclusion and acknowledgement section. Here they are mixe ed which is not acceptable)

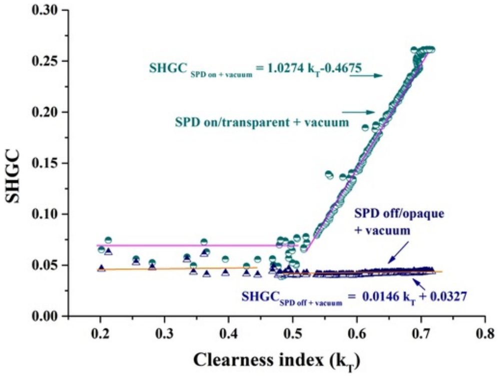

Fig. 9 Dependency of transmitted solar energy through SPD glazing on and off condition with clearness index.

alt-text: Fig. 9: (Please use the attached figure for Figure 9 for clarity)

Table 4 Yearly usable single transmitted energy value for SPD-vacuum transparent and opaque state.

alt-text: Table 4:

	Azimuthal direction	SPD on (38% transparent)+vacuum transmitted solar energy (W/m2)	SPD off (2% transparent)+vacuum transmitted solar energy (W/m2)	Clearness index
	North	21	11	0.7
	South	21	11	0.5
Vertical plane SPD-vacuum glazing	East	21	11	0.6
	West	21	11	0.6
	North east	21	11	0.6
	North west	21	11	0.6

Acknowledgements

The authors would also like to thank the anonymous reviewers for their constructive comments that helped to improve the manuscript.

The work described in this paper was supported by the Graduate Research Education Programme of the Higher Education Authority, Ireland.

References (Please keep the section 5 conclusion and acknowledgements will come after conclusion section)

[1] Roadmap 2050 Volume 1: Technical and EconomicAnalysis, accessed online in May 2016 at⟨http://www.roadmap2050.eu/attachments/files/Volume1_ExecutiveSummary.pdf⟩

[2] Energy Performance of Buildings Directive recast2010/31/EU ~~(2010).~~2010.~~(~~areas/buildings/EPBD_Recast/EPBD_recast_19May2010.pdf>⟩⟨⟩.

[3] F. Favoino, F. Fiorito, A. Cannavale, G. Ranzi and M. Overend, Optimal control and performance of photovoltachromic switchable glazing for building integration in temperate climates, ~~Applied~~Appl. *Energy* **178**, 2016, 943–961.

[4] F. Favoino, M. Overen and Q. Jin, The optimal thermo-optical properties and energy saving potential of adaptive glazing technologies, ~~Applied~~Appl. *Energy* **156**, 2015, 1–15.

[5] A. Seeboth, J. Schneider and A. Patzak, Materials for intelligent sun protecting glazing, ~~Solar~~Sol. *Energy* ~~Materials and Solar~~ Mater. Sol. *Cells* **60**, 2000, 263–277.

[6] G. Gorgolis and D. Karamanis, Solar energy materials for glazing technologies, ~~Solar~~Sol. *Energy* ~~Materials and Solar~~ Mater. Sol. *Cells* **144**, 2016, 559–578.

[7] R. Baetens, B.P. Jelle and A. Gustavsen, Properties, requirements, and possibilities of smart windows for dynamic daylight and solar energy control in buildings: ~~A~~a state-of-the-art review, ~~Solar~~Sol. *Energy* ~~Materials & Solar~~ Mater. Sol. *Cells* **94**, 2010, 87–105.

[8] B.P. Jelle, A. Hynd, A. Gustavsen, D. Arasteh, H. Goudey and R. Hart, Fenestration of today and tomorrow: ~~A~~a state-of-the-art review and future research opportunities, ~~*Solar*~~*Sol. Energy* ~~*Materials & Solar*~~ *Mater. Sol. Cells* **96**, 2012, 1–28.

[9] C.M. Lampert, Towards large-area photovoltaic nanocells: experiences learned from smart window technology, ~~*Solar*~~*Sol. Energy* ~~*Material & Solar cells*~~*Mater. Sol. Cells* **11**, 1984, 1–27.

[10] C.M. Lampert, Smart switchable glazing for solar energy and daylight control, ~~*Solar*~~*Sol. Energy* ~~*Materials & Solar*~~ *Mater. Sol. Cells* **52**, 1998, 207–221.

[11] A. Georg and A. Georg, Electrochromic device with a redox electrolyte, ~~*Solar*~~*Sol. Energy* ~~*Materials & Solar*~~ *Mater. Sol. Cells* **93**, 2009, 1329–1337.

[12] R. Vergaz, J.M.S.N. Pena, D. Barrios, C. Va´zquez and P.C. Lallana, Modelling and electro-optical testing of suspended particle devices, ~~*Solar*~~*Sol. Energy* ~~*Materials & Solar*~~ *Mater. Sol. Cells* **92**, 2008, 1483–1487.

[13] D. Barrios, R. Vergaz, J.M.S.N. Pena, C.G. Granqvist and G.A. Niklasson, Toward a quantitative model for suspended particle devices: optical scattering and absorption coefficients, ~~*Solar*~~*Sol. Energy* ~~*Materials & Solar*~~ *Mater. Sol. Cells* **111**, 2013, 115–122.

[14] D. Barrios, R. Vergaz, J.M.S.N. Pena, B.G. Cámara, C.G. Granqvist and G.A. Niklasson, Simulation of the thickness dependence of the optical properties of suspended particle devices, ~~*Solar*~~*Sol. Energy* ~~*Materials & Solar*~~ *Mater. Sol. Cells* **143**, 2015, 613–622.

[15] A. Ghosh, B. Norton and A. Duffy, Measured overall heat transfer coefficient of a suspended particle device switchable glazing, ~~*Applied*~~*Appl. Energy* **159**, 2015, 362–369.

[16] D.J. Gardiner, S.M. Morris and H.J. Coles, High-efficiency multistable switchable glazing using smectic A liquid crystals, ~~*Solar*~~*Sol. Energy* ~~*Materials & Solar*~~ *Mater. Sol. Cells* **93**, 2009, 301–306.

[17] C.M. Lampert, Chromogenic smart materials, ~~*Materials*~~*Mater. Today* **7**, 2004, 28–35.

[18] V. Costanzo, G. Evola and L. Marletta, Thermal and visual performance of real and theoretical thermochromic glazing solutions for office buildings, ~~*Solar*~~*Sol. Energy* ~~*Materials and Solar*~~ *Mater. Sol. Cells* **149**, 2016, 110–120.

[19] M.E.A. Warwick, I. Ridley and R. Binions, The effect of variation in the transition hysteresis width and gradient in thermochromic glazing systems, ~~*Solar*~~*Sol. Energy* ~~*Materials and Solar*~~ *Mater. Sol. Cells* **140**, 2015, 253–265.

[20] P. Nitz and H. Hartwig, Solar control with thermotropic layers, ~~*Solar*~~ *Sol. Energy* **79**, 2005, 573–582.

[21] A. Weber and K. Resch, Thermotropic glazings for overheating protection, *Energy Procedia* **30**, 2012, 471–477.

[22] F. Goia, Thermo-physical behaviour and energy performance assessment of PCM glazing system configurations: ~~A~~a numerical analysis, ~~*Frontiers of Architectural Research*~~*Front. Archit. Res.* **1**, 2012, 341–347.

[23] F. Goia, M. Zinzi, E. Carnielo and V. Serra, Spectral and angular solar properties of a PCM-filled double glazing unit, *Energy* ~~*and Buildings*~~*Build.* **87**, 2015, 302–312.

[24] F. Goia, M. Perino and V. Serra, Experimental analysis of the energy performance of a full-scale PCM glazing prototype, ~~*Solar*~~*Sol. Energy* **100**, 2014, 217–233.

[25] F. Goia, M. Perino and V. Serra, Improving thermal comfort conditions by means of PCM glazing systems, *Energy* ~~*and Buildings*~~*Build.* **60**, 2013, 442–452.

[26] A. Georg, W. Graf, R. Neumann and V. Wittwer, Stability of gasochromic WO_3 films, ~~*Solar*~~*Sol. Energy* ~~*Materials & Solar*~~ *Mater. Sol. Cells* **63**, 2000, 165–176.

[27] W. Feng, L. Zou, G. Gao, G. Wu, J. Shen and W. Li, Gasochromic smart window: optical and thermal properties, energy simulation and feasibility analysis, ~~*Solar*~~*Sol. Energy* ~~*Materials and Solar*~~ *Mater. Sol. Cells* **144**, 2016, 316–323.

[28] C. Buratti and E. Moretti, Experimental performance evaluation of aerogel glazing systems, ~~*Applied*~~*Appl. Energy* **97**, 2012, 430–437.

[29] J.M. Schultz, K.I. Jensen and F.H. Kristiansen, Super insulating aerogel glazing, ~~*Solar*~~*Sol. Energy* ~~*Materials and Solar*~~ *Mater. Sol. Cells* **89**, 2005, 275–285.

[30] Y. Fang, T.J. Hyde, F. Arya, N. Hewitt, P.C. Eames, B. Norton and S. Miller, Indium alloy-sealed vacuum glazing development and context, ~~*Renewable and Sustainable*~~ *Renew. Sustain. Energy* ~~*Reviews*~~*Rev.* **37**, 2014, 480–501.

[31] S. Papaefthimiou, G. Leftheriotis, P. Yianoulis, T.J. Hyde, P.C. Eames, Y. Fang, P.Y. Pennarun and P. Jannasch, Development of electrochromic evacuated advanced glazing, *Energy* ~~*and Buildings*~~*Build.* **38**, 2006, 1455–1467.

[32] A. Ghosh, B. Norton and A. Duffy, First outdoor characterisation of a PV powered suspended particle device switchable glazing, ~~*Solar*~~*Sol. Energy* ~~*Materials & Solar*~~ *Mater. Sol. Cells* **157**, 2016, 1–9.

[33] A. Ghosh, B. Norton and A. Duffy, Behaviour of a SPD switchable glazing in an outdoor test cell with heat removal under varying weather conditions, ~~Applied~~Appl. *Energy* **180**, 2016, 695–706.

[34] A. Ghosh, B. Norton and A. Duffy, Daylighting performance and glare calculation of a suspended particle device switchable glazing, ~~Solar~~Sol. *Energy* **132**, 2016, 114–128.

[35] A. Ghosh, B. Norton and A. Duffy, Measured thermal & daylight performance of an evacuated glazing using an outdoor test cell, ~~Applied~~Appl. *Energy* **177**, 2016, 196–203.

[36] A. Ghosh, B. Norton and A. Duffy, Measured thermal performance of a combined suspended particle switchable device evacuated glazing, ~~Applied~~Appl. *Energy* **169**, 2016, 469–480.

[37] P.A. Waide and B. Norton, Variation of insolation transmission with glazing plane position and sky conditions, *ASME* ~~Journal of Solar~~ J. Sol. *Energy* ~~Engineering~~Eng. **125**, 2003, 182–189.

[38] M.J. Brandemuehl and W.A. Beckman, Transmission of diffuse radiation through CPC and flat-plate collector glazings, ~~Solar~~Sol. *Energy* **24**, 1980, 511–513.

Highlights

- Correlation of SPD-vacuum glazing transmittance and clearness index has been calculated.
- Transmitted solar energy and SHGC was evaluated for different clearness index.
- Single glazing transmittance value was recommended below 0.5 clearness index.
- Maximum transmitted SE was 76% higher in SPD-vacuum transparent state than opaque.

Queries and Answers

Query:

Your article is registered as a regular item and is being processed for inclusion in a regular issue of the journal. If this is NOT correct and your article belongs to a Special Issue/Collection please contact j.alwyn@elsevier.com immediately prior to returning your corrections.

Answer: It is a regular item